

AD-A169 178

HDL-TR-2079

May 1986

**Transmission Through Ferrite Samples at
Submillimeter Frequencies**

by Clyde A. Morrison
Barbara J. Bencivenga
George J. Simonis

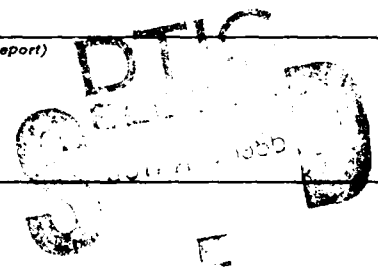


**U.S. Army Laboratory Command
Harry Diamond Laboratories
Adelphi, MD 20783-1197**

UNCLASSIFIED

SECURITY CLASSIFICATION OF THIS PAGE (When Data Entered)

REPORT DOCUMENTATION PAGE		READ INSTRUCTIONS BEFORE COMPLETING FORM	
1. REPORT NUMBER HDL-TR-2079	2. GOVT ACCESSION NO.	3. RECIPIENT'S CATALOG NUMBER	
4. TITLE (and Subtitle) Transmission Through Ferrite Samples at Submillimeter Frequencies		5. TYPE OF REPORT & PERIOD COVERED Technical Report	
		6. PERFORMING ORG. REPORT NUMBER	
7. AUTHOR(s) Clyde A. Morrison Barbara J. Bencivenga George J. Simonis		8. CONTRACT OR GRANT NUMBER(s)	
9. PERFORMING ORGANIZATION NAME AND ADDRESS Harry Diamond Laboratories 2800 Powder Mill Road Adelphi, MD 20783-1197		10. PROGRAM ELEMENT, PROJECT, TASK AREA & WORK UNIT NUMBERS Program Element: 611102A DA Project: 1L161102AH44	
11. CONTROLLING OFFICE NAME AND ADDRESS U.S. Army Laboratory Command 2800 Powder Mill Road Adelphi, MD 20783-1145		12. REPORT DATE May 1986	
		13. NUMBER OF PAGES 21	
14. MONITORING AGENCY NAME & ADDRESS (if different from Controlling Office)		15. SECURITY CLASS. (of this report) UNCLASSIFIED	
		15a. DECLASSIFICATION/DOWNGRADING SCHEDULE	
16. DISTRIBUTION STATEMENT (of this Report) Approved for public release; distribution unlimited.			
17. DISTRIBUTION STATEMENT (of the abstract entered in Block 20, if different from Report)			
18. SUPPLEMENTARY NOTES HDL Project: AE1557 AMS Code: 611102.H440011			
19. KEY WORDS (Continue on reverse side if necessary and identify by block number) Magnetic resonance Ferrite Fourier transform spectroscopy Submillimeter waves			
20. ABSTRACT (Continue on reverse side if necessary and identify by block number) A theoretical analysis is presented of the transmission spectra of thin magnetized ferrite slabs. The energy range chosen was $1 < \bar{\nu} < 120 \text{ cm}^{-1}$ ($30 \text{ GHz} < f < 3600 \text{ GHz}$). The magnetic field was assumed to lie in the plane of the ferrite slab, and the incident electromagnetic radiation was polarized parallel and perpendicular to the magnetic field. For measurements of the magnetic properties near resonance, we show that extremely stable sources are required. However, we show that meaningful measurements can be made far from magnetic resonances using a conventional Fourier transform spectrometer.			



UNCLASSIFIED

CONTENTS

	<u>Page</u>
1. INTRODUCTION	5
2. THEORY	6
3. DISCUSSION AND CONCLUSION	15
ACKNOWLEDGEMENTS	16
LITERATURE CITED	16
DISTRIBUTION	17

FIGURES

1. Ferromagnetic resonance for a plane wave in an infinite medium characterized by $\mu_e = \mu_{e1} + i\mu_{e2}$, $\epsilon = \epsilon_1 + i\epsilon_2$, $n = \sqrt{\epsilon\mu_e} = n_1 + in_2$	10
2. Increase in measured linewidth as a function of thickness of ferrite slab. External magnetic field is 50,000 gauss	11
3. Shift in resonance frequency as a function of thickness of ferrite slab. External magnetic field, H_0 , is 50,000 gauss	11
4. Power transmission coefficient for 2- μ m-thick ferrite slab. External magnetic field, H_0 , is 50,000 oersteds	12
5. Power transmission coefficient for 10- μ m-thick ferrite slab. External magnetic field, H_0 , is 50,000 oersteds	12
6. Power transmission coefficient for a 40- μ m-thick ferrite slab. External magnetic field, H_0 , is 50,000 oersteds	12
7. Power transmission coefficient for 70- μ m-thick ferrite slab. External magnetic field, H_0 , is 50,000 oersteds	12
8. Power transmission coefficient for 100- μ m-thick ferrite slab. External magnetic field, H_0 is 50,000 oersteds	13
9. Experimental values of ϵ_2	14
10-13. Power transmission coefficient ($E \parallel H_0$ solid, $E \perp H_0$ dotted) for 1-mm-thick sample	14-15
14. Power transmission coefficient ($E \parallel H_0$ solid, $E \perp H_0$ dashed) for 1-cm-thick sample	15

A-1

1. INTRODUCTION

Because of an increased technological interest in materials to be used in the submillimeter region and higher frequencies, it has become important to measure the properties of useful materials at these frequencies. The complex dielectric constant of a number of materials has been measured in the 4 to 20 cm^{-1} range,¹ but very little has been reported on the magnetic properties of ferrites or other ferromagnetic materials.

In this report we present a theoretical analysis applicable to the measurement of the magnetic properties of materials in the energy range $1 \text{ cm}^{-1} < \bar{\nu} < 120 \text{ cm}^{-1}$ ($30 \text{ GHz} < f < 3600 \text{ GHz}$). The analysis consists of an investigation of the transmission of a ferrite slab magnetized in the plane of the slab with the electromagnetic wave polarized parallel or perpendicular to the magnetic field. The direction of propagation is perpendicular to the plane of the slab.

The first case analyzed is for ferromagnetic resonance occurring in the range $3 \text{ cm}^{-1} < \bar{\nu} < 7 \text{ cm}^{-1}$. This range of energy is somewhat hypothetical for conventional ferrites because of the requirement of extremely large magnetic fields (50,000 gauss). Nevertheless, an investigation of resonance at these frequencies does illustrate the resolution requirements on any spectrum analyzer that might be used in the measurements. However, the resonance of hexagonal ferrites does occur at submillimeter frequencies for moderate fields, and the analysis given is useful for these materials. A number of antiferromagnetic materials have their resonances at very high frequencies and at moderate external magnetic fields. These materials have received little attention as to their possible application in the submillimeter region. This analysis should be useful with possibly slight modification.

The second aspect of this report is the investigation of the magnetic effects far from ferromagnetic resonance ($\bar{\nu} \gg \bar{\nu}_{\text{res}}$). Because of the application of a number of ferrites at microwave frequencies, good quality materials are available in that frequency range. These materials have low internal fields, and magnetic resonance is determined predominately by the application of an external field. Little is known of the properties of these latter materials in the frequency band from 1 to 20 cm^{-1} . The results predicted here use the values characterizing the ferrite at X-band and may be altered when such quantities as the dielectric constants are better determined.

¹George J. Simonis, Joseph P. Sattler, Terrance L. Worchesky, and Richard P. Leavitt, Characterization of Near-Millimeter Wave Materials by Means of Non-Dispersive Fourier Transform Spectroscopy, *J. Infrared and Mill. Waves*, 5 (1984), 57. (This reference reports the measured complex dielectric constant of TT2-111, the prototype ferrite used here.) See also George J. Simonis, Index to the Literature Dealing with the Near-Millimeter Wave Properties of Materials, *Int. J. Infrared and Mill. Waves*, 3 (1982), 439 (170 articles referenced).

2. THEORY

In a previous report,² an expression for the effective permeability, μ_e , was derived for a lossless medium. In the appendix of that report, the expressions for μ and κ were derived using Gilbert's³ damping to give ($e^{-i\omega t}$ assumed time dependence)

$$\mu_{\pm} = 1 \mp \frac{\gamma 4\pi M}{\omega \pm i\gamma\Delta H \mp \gamma H_0} \quad (1)$$

$$\mu_{\pm} = \mu \pm i\kappa \quad ,$$

with

$$B_x \pm iB_y = \mu_{\pm} (H_x \pm iH_y)$$

and

$$B_x = \mu H_x + i\kappa H_y \quad , \quad B_y = \mu H_y - i\kappa H_x \quad ,$$

where

$4\pi M$ = the saturation magnetization,

γ = the gyromagnetic ratio,

ΔH = one-half the full line width at half maximum,

H_0 = the external field along the z direction.

The μ_{\pm} in equation (1) corresponds to the permeability seen by right or left circular polarized waves propagating in the direction of the external field in an infinite medium. The experimental results are usually given as the full line width at half maximum, δH . Then ΔH in equation (1) is given by $\Delta H = \delta H/2$. If the external magnetic field is applied along a principal axis, the magnetic anisotropy can then be taken into account by letting $H_0 \rightarrow H_0 + H_A$, where H_A is the effective anisotropy field.⁴ If we assume that we have a

²Clyde A. Morrison, A. F. Hansen, and K. M. Sorenson, Theoretical Analysis of Nonreciprocal Electromagnetic Surface Wave Devices, Harry Diamond Laboratories, HDL-TR-2017 (September 1983).

³T. A. Gilbert, Armour Research Foundation, Rept. No. 11 (25 January 1955).

⁴W. H. Von Aulock, ed., Handbook of Microwave Ferrite Materials, Academic Press, New York (1965), 464.

plane wave with E parallel to the field H_0 and in the plane of a slab of thickness, a , the relative amplitude of the transmitted wave is

$$T_{a\parallel} = \frac{e^{-ika}}{\cos(ka\sqrt{\epsilon\mu_e}) - \frac{i}{2} \left(z_e + \frac{1}{z_e} \right) \sin(ka\sqrt{\epsilon\mu_e})} , \quad (2)$$

where

$$k = \frac{\omega}{c} ,$$

$$k = 2\pi\bar{\nu} ,$$

$$\mu_e = \frac{\mu^2 - k^2}{\mu} ,$$

$$z_e = \sqrt{\mu_e/\epsilon} ,$$

and ϵ is the dielectric constant. In equation (2), k is always real, but ϵ and μ_e are, in general, complex.

In the derivation of equation (2), the slab is assumed to lie in the y - z plane and to be of thickness a . The wave equations for E_z in the two regions were taken as

$$\frac{d^2}{dx^2} E_z = -k^2 E_z \quad \text{in free space} ,$$

$$a < x , \quad x < 0 ,$$

and

$$\frac{d^2}{dz^2} E_z = -k^2 \epsilon \mu_e E_z \quad \text{in the ferrite} ,$$

$$0 < x < a .$$

The result given in equation (2) was obtained by using the general solution to equation (3) and boundary conditions on E_z and H_y at the interfaces $x = 0$ and $x = a$. The amplitude transmission coefficient for plane waves polarized with $E \perp H_0$ (the z -axis) is obtained by letting $\mu_e \rightarrow 1$ in equation (2), or

$$T_{a\perp} = \frac{e^{-ika}}{\cos(ka\sqrt{\epsilon}) - \frac{i}{2} \left(\sqrt{\epsilon} + \frac{1}{\sqrt{\epsilon}} \right) \sin(ka\sqrt{\epsilon})} . \quad (4)$$

In the derivation of equation (4), the field E was assumed to be polarized along the y-direction, and the wave equation inside the ferrite is

$$\frac{d^2}{dx^2} E_y = -k^2 \epsilon E_y \quad (5)$$

In all the equations given above, ϵ and μ_e are, in general, complex.

Measurements are generally made on the power transmitted which is $|T_a|^2$ in either equation (2) or (4). If we assume that the thickness, a , is very small, then

$$\cos(ka\sqrt{\epsilon\mu_e}) \sim 1 \quad ,$$

and

$$\sin(ka\sqrt{\epsilon\mu_e}) \sim ka\sqrt{\epsilon\mu_e} \quad .$$

And, from equation (2),

$$T_a = \frac{1}{1 - \frac{i}{2}(\epsilon + \mu_e)ka} \quad (6)$$

The power transmitted, $T_p = |T_a|^2$, becomes

$$T_p = \frac{1}{1 + (\epsilon_2 + \mu_{e2})ka} \quad (7)$$

where

$$\epsilon = \epsilon_1 + i\epsilon_2 \quad ,$$

and

$$\mu_e = \mu_{e1} + i\mu_{e2} \quad .$$

The effective permeability, μ_e , given in equation (2) is the permeability as seen by a plane wave propagating in the x-y plane polarized with E in the z direction. Using the result of equation (1) and the expression for μ_e given in equation (2), we obtain

$$\mu_e = \frac{(H_1 - B)(H_1 + B) + \Delta H^2 + i(2B)\Delta H}{(H_1 - H_2)(H_1 + H_2) + \Delta H^2 + i(B + H)\Delta H} \quad (8)$$

where

$$H_1 = \frac{\omega}{\gamma} ,$$

$$H_2 = \sqrt{BH} ,$$

$$B = H + 4\pi M ,$$

$$\gamma = [8.795 \times 10^6 \text{ radians/(second-oersted)}]g ,$$

and

$$g = \text{effective } g \text{ factor (generally } \sim 2) .$$

The complex index of refraction, n , is given by

$$n = \sqrt{\epsilon\mu_e} ,$$

$$n = n_1 + in_2 ,$$

and

$$\epsilon = \epsilon_1 + i\epsilon_2 ,$$

$$\mu_e = \mu_{e1} + i\mu_{e2} .$$

The components of the complex μ_e and n are shown in figure 1 for an applied field of 50,000 oersteds. The parameters of the ferrite (see TT2-111, Von Aulock⁴) are

$$4\pi M_s = 5000 \text{ gauss} ,$$

$$\Delta H = 67.5 \text{ oersteds (experimental full half power width = 135.0 oersteds)},$$

$$g = 2.08 ,$$

$$\epsilon_1 = 12.5 ,$$

and

$$\epsilon_2 = 0.0125 .$$

⁴W. H. Von Aulock, ed., Handbook of Microwave Ferrite Materials, Academic Press, New York (1965), 464.

The linewidth of the ferrite chosen for figure 1 is characteristic of the linewidths observed at microwave frequencies. It is quite possible that this width will not change significantly at higher frequencies. Thus, to observe resonance directly at these high frequencies ($\bar{\nu} > 5 \text{ cm}^{-1}$), the spectrometer will have to have a very high resolving power. Resonance could most readily be directly observed with a stabilized oscillator and by sweeping the magnetic field through resonance, as is done at microwave frequencies.⁵

The results shown in figure 1 are for an infinite medium. When the sample is of finite extent, the boundaries of the ferrite affect the resonance condition. In fact, for different shaped samples whose dimensions are small compared to the wavelength, Kittel⁶ shows that the resonance condition varies considerably with the shape of the sample. Using the result of equation (8), we obtain

$$\mu_{e2} = \frac{4\pi M(B^2 + H_1^2 + \Delta H^2)\Delta H}{(H_1^2 - H_2^2 + \Delta H^2)^2 + (B + H)^2 \Delta H^2} \quad (9)$$

The result given in equation (9) was substituted into equation (7), and the minimum values of T_p were found for a range of slab thicknesses a , such that $ka < 1$. The increase in the linewidth of the power transmitted is shown in figure 2 for the same parameters used in the calculations of figure 1. As can be seen, the linewidth increases quite rapidly with slab thickness (slope $\sim 10.0 \text{ cm}^{-1}/\text{cm}$). The frequency at resonance also shifts with slab thickness. This shift is important in determining the gyromagnetic ratio or, equivalently, the effective g value ($\gamma = g(1.3998 \times 10^6) \text{ Hz/oersted}$).

The shift of the peak at maximum absorption is shown in figure 3 for the same range of thickness as shown in figure 2. Also, the same ferrite was chosen. For the ferrite chosen in figure 3, the shift in frequency at resonance is seen to be negligible for $a < 10 \mu\text{m}$. For thicker ferrite samples, the behavior near resonance becomes very complicated, and the extraction of the properties of the material that determine resonance is difficult or

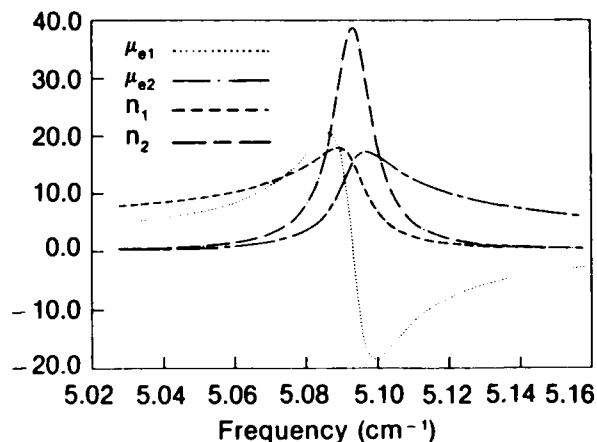


Figure 1. Ferromagnetic resonance for a plane wave in an infinite medium characterized by $\mu_e = \mu_{e1} + i\mu_{e2}$, $\epsilon = \epsilon_1 + i\epsilon_2$, $n = \sqrt{\epsilon\mu_e} = n_1 + in_2$. Parameters characterizing ferrite TT2-111 are $4\pi M_s = 5000$ gauss, $\delta H = 135$ oersteds, $g_{\text{eff}} = 2.08$, $\epsilon_1 = 12.5$, and $\epsilon_2 = 0.0125$.

⁵Joseph Nemanich, Measurement of Narrow Magnetic Resonance Linewidths, Harry Diamond Laboratories, HDL-TR-1246 (10 August 1964).

⁶C. Kittel, Introduction to Solid State Physics, Wiley and Sons, New York (1976).

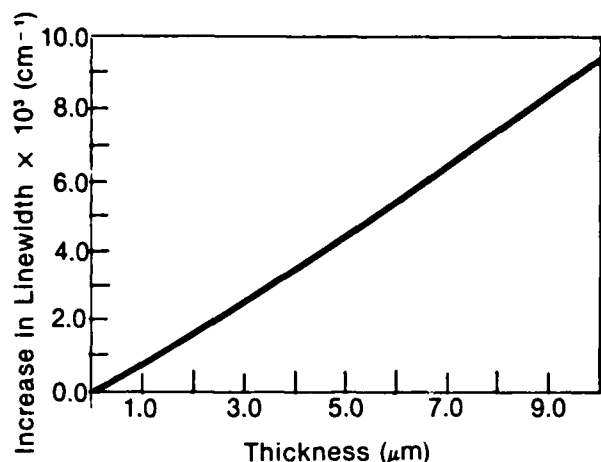


Figure 2. Increase in measured linewidth as a function of thickness of the ferrite slab. External magnetic field is 50,000 gauss. Parameters characterizing ferrite are given in figure 1.

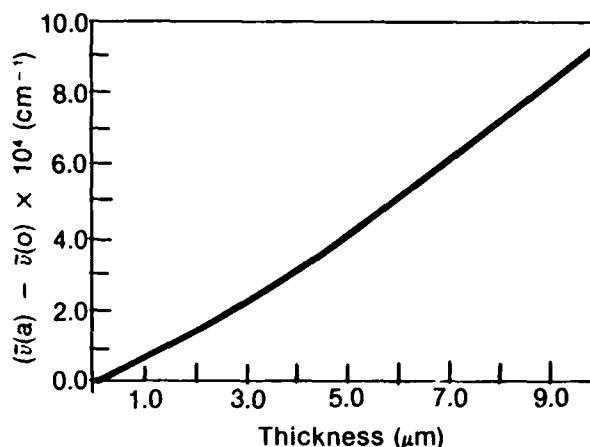


Figure 3. Shift in resonance frequency as a function of thickness of ferrite slab. External magnetic field, H_0 , is 50,000 gauss. Parameters characterizing ferrite are given in figure 1.

impossible. To illustrate the effect of increasing thickness on the transmitted power through a ferrite slab, several thicknesses were chosen, and the results are shown in figures 4 through 8. All these figures are for the same ferrite (TT2-111). In figure 4, the ferrite thickness is chosen by using the results of figures 2 and 3. For a 2- μm -thick sample, the increase in linewidth is approximately 0.3 cm^{-1} , and the shift is approximately $2 \times 10^{-3} \text{ cm}^{-1}$. This small shift is negligible, but the increase in linewidth may be significant, depending on the desired precision of the experimental results. Figure 5 gives the transmission of a 10- μm -thick sample as a function of frequency. Pronounced asymmetry of the resonance line has begun to appear due to an increase, at magnetic resonance, in the optical thickness of the sample. As the thickness is increased to 40 μm , the entire transmission becomes distorted so much that resonance behavior is obliterated, as shown in figure 6. Figures 7 and 8 are for 70- and 100- μm -thick samples and illustrate the complicated behavior of the transmission near ferromagnetic resonance. These latter results illustrate the difficulty, if not the impossibility, of extracting the proper ties of the ferromagnetic material near resonance if the samples are too thick.

For most of the ferrites developed for use at microwave frequencies, the external magnetic field required for resonance at submillimeter wavelengths ($5 < \nu < 100 \text{ cm}^{-1}$) is very large ($H_0 \sim 50,000$ oersteds in the previous examples). Such magnetic fields are unobtainable in most laboratories. Thus, it is important whether or not meaningful measurements can be made in the region $f \gg \gamma(H_2^2 - \Delta H^2)^{1/2}$ (approximately the frequency of resonance in infinite media). For very high frequency (H_1 larger than all other quantities in equation (8)),

$$\mu_e \approx 1 - \frac{4\pi MB}{H_1^2} + i \frac{4\pi M\Delta H}{H_1^2}, \quad (10)$$

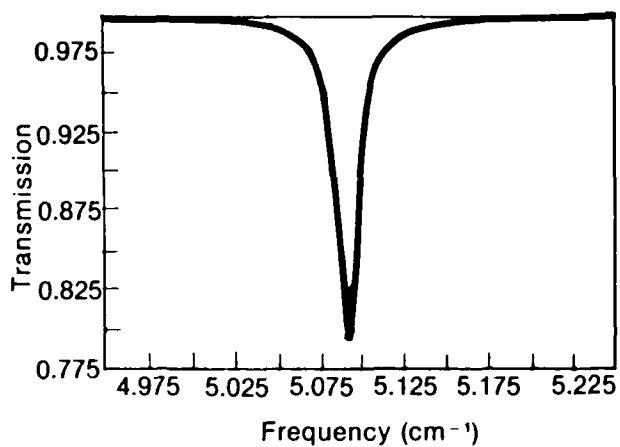


Figure 4. Power transmission coefficient for 2- μm -thick ferrite slab. External magnetic field, H_0 , is 50,000 oersteds. Parameters characterizing ferrite are given in figure 1.

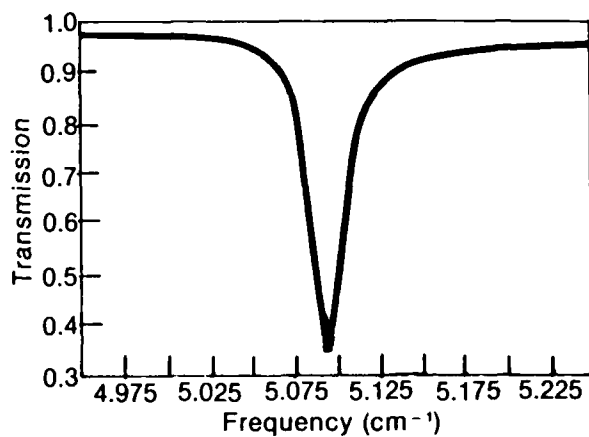


Figure 5. Power transmission coefficient for 10- μm -thick ferrite slab. External magnetic field, H_0 , is 50,000 oersteds. Parameters characterizing ferrite are given in figure 1.

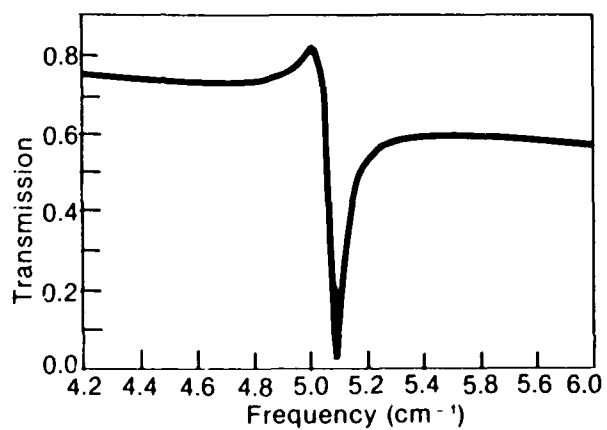


Figure 6. Power transmission coefficient for 40- μm -thick ferrite slab. External magnetic field, H_0 , 50,000 oersteds. Parameters characterizing ferrite are given in figure 1.

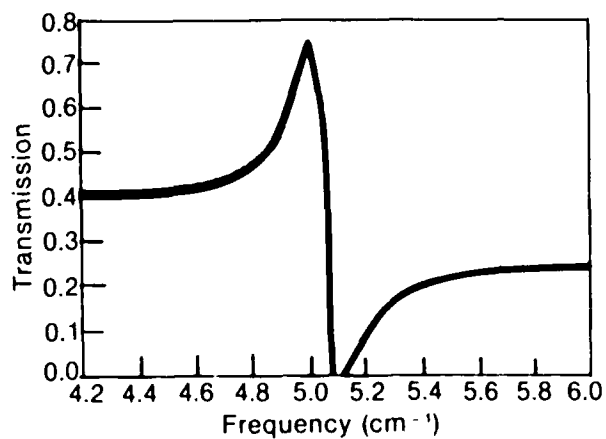


Figure 7. Power transmission coefficient for 70- μm -thick ferrite slab. External magnetic field, H_0 , is 50,000 oersteds. Parameters characterizing ferrite are given in figure 1.

and the index of refraction is much smaller than when near ferromagnetic resonance. Thus, much thicker slabs of ferrite can be used in the measurements at these higher frequencies. Even with thicker samples, the frequency intervals between maxima and minima of the transmission ($\Delta\bar{\nu} \sim 1/an_1$) are resolvable so that the complex index of refraction can be extracted from the data. Further, the complex dielectric constant can be measured using the result given in equation (4) ($T_{p\perp} = |T_{a\perp}|^2$), and this result can be used to extract μ_e by using measurements of $T_{p\parallel}$ given by equation (2), ($T_{p\parallel} = |T_{a\parallel}|^2$).

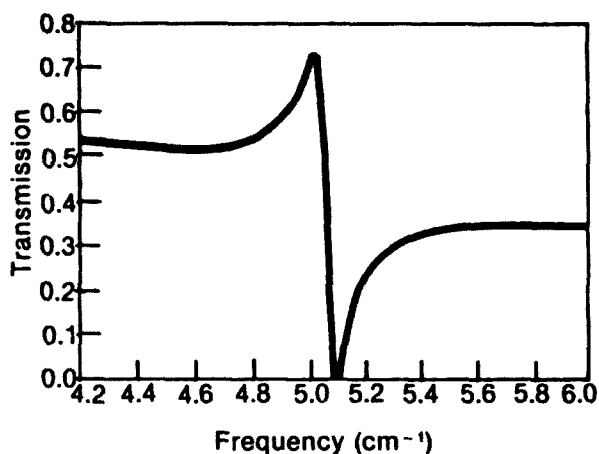


Figure 8. Power transmission coefficient for 100- μm -thick ferrite slab. External magnetic field, H_0 , is 50,000 oersteds. Parameters characterizing ferrite are given in figure 1.

For the ferrite characterized in figure 1, the transmitted power was determined for a slab of thickness $a = 1$ mm using equation (4) and the results shown in figure 9. The effect

of the periodic oscillations ("channel spectrum") is very evident. In the lower frequency range ($\bar{\nu} < 7 \text{ cm}^{-1}$), the differences between $T_{p\parallel}$ and $T_{p\perp}$ are distinguishable. Below 2.5 cm^{-1} , ferromagnetic resonance effects are evident. Thus, in the range $2.5 \text{ cm}^{-1} < \bar{\nu} < 7 \text{ cm}^{-1}$, the dielectric constant $\bar{\epsilon}$ can be determined using the transmission curve, $T_{p\perp}$. At a higher frequency, $\bar{\nu} > 5 \text{ cm}^{-1}$, the dielectric losses increase significantly. The measured values of ϵ_2 ($\epsilon = \epsilon_1 + i\epsilon_2$) for the ferrite TT2-111 are given in figure 9 as reported by Simonis et al.¹ The region $0 < \bar{\nu} < 7 \text{ cm}^{-1}$ is estimated, but the region $7 < \bar{\nu} < 17.5 \text{ cm}^{-1}$ has been measured experimentally. The solid lines in figure 9 are approximate fits to the data in the two regions. The variation of ϵ^2 with $\bar{\nu}$ in the region $0 < \bar{\nu} < 5 \text{ cm}^{-1}$ has been checked for the cases given in figures 4 through 8, and it has negligible effect. However, figure 10 shows the transmission through a slab of 1 mm with $\epsilon^2 = 0.0125$, and figure 11 shows the results when the data of figure 9 are used. As can be seen, the effect of the increase in ϵ_2 with frequency is significant and must be considered in the higher frequency calculations. For the same thickness samples, the transmission was calculated for external magnetic fields of 10,000 and 15,000 oersteds, and the results are shown in figures 12 and 13. The range of frequencies for $\bar{\nu} \gg \gamma H$ ($\bar{\nu} > 5 \text{ cm}^{-1}$), over which the two curves $T_{p\parallel}$ and $T_{p\perp}$ increase with magnetic field, is as would be expected from equation (10). With the results given in figures 11, 12, and 13 viewed as experimental data, it seems reasonable to assume that the parameters $4\pi M$ and γ can be

¹George J. Simonis, Joseph P. Sattler, Terrance L. Worchesky, and Richard P. Leavitt, Characterization of Near-Millimeter Wave Materials by Means of Non-Dispersive Fourier Transform Spectroscopy, *J. Infrared and Mill. Waves*, 5 (1984), 57. (This reference reports the measured complex dielectric constant of TT2-111, the prototype ferrite used here.) See also George J. Simonis, Index to the Literature Dealing with the Near-Millimeter Wave Properties of Materials, *Int. J. Infrared and Mill. Waves*, 3 (1982), 439 (170 articles referenced).

determined by using equation (10) in conjunction with experimental data. The transmission coefficient for a 1-cm-thick sample (TT2-111) is shown in figure 14. Despite the complicated appearance of the curves, the effective index of refraction can easily be extracted from the data for the entire range of frequencies ($3 \text{ cm}^{-1} < \bar{\nu} < 6 \text{ cm}^{-1}$).

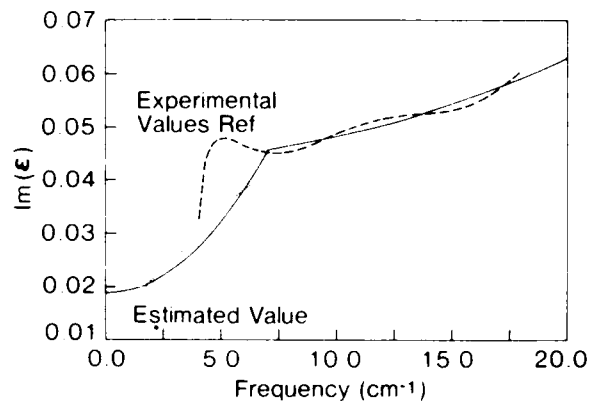


Figure 9. Experimental values of ϵ_2 . The ϵ_2 values for 0 to 7.5 cm^{-1} are estimated, and the values $7.5 < f < 17.5 \text{ cm}^{-1}$ are reported by Simonis et al. Solid lines are approximate fits to the experimental data and are used in the computation.

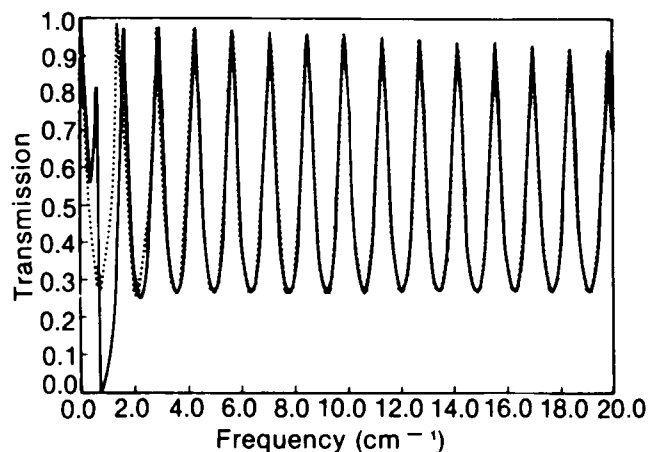


Figure 10. Power transmission coefficient ($E \parallel H_0$ solid, $E \perp H_0$ dotted) for 1-mm-thick sample. External field, H_0 , is 5000 oersteds. Parameters characterizing ferrite are given in figure 1.)

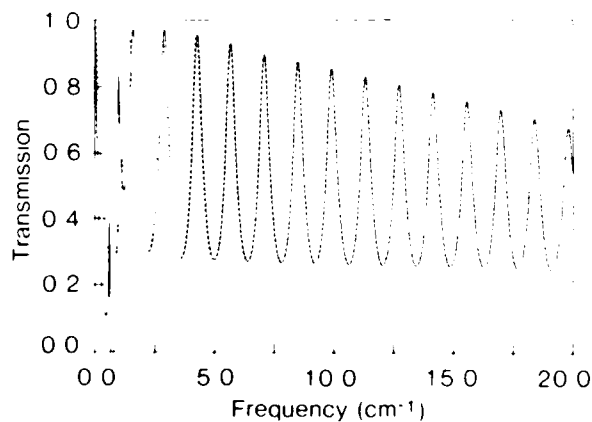


Figure 11. Power transmission coefficient ($E \parallel H_0$ solid, $E \perp H_0$ dashed) for 1-mm-thick sample. External field, H_0 , is 5000 oersteds. Parameters characterizing ferrite are given in figure 1, except for value of ϵ_2 . Values of ϵ_2 are taken from the fit to experimental data given in figure 9.

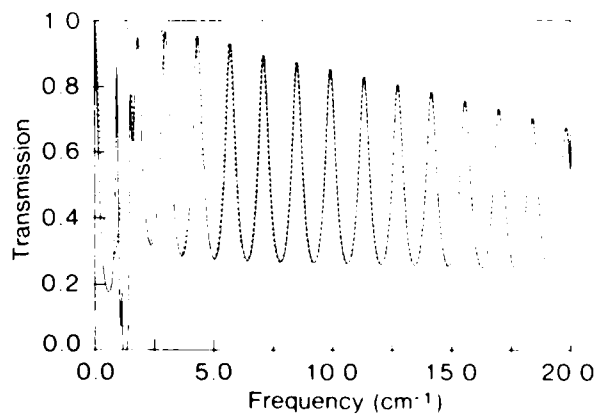


Figure 12. Power transmission coefficient ($E \parallel H_0$ solid, $E \perp H_0$ dashed) for 1-mm-thick sample. Magnetic field, H_0 , is 10,000 oersteds. Parameters characterizing ferrite are given in figure 1. (See fig. 9 for ϵ_2 .)

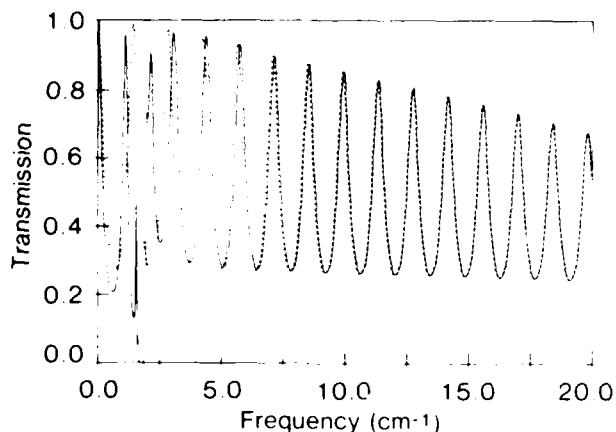


Figure 13. Power transmission coefficient ($E \parallel H_0$ solid, $E \perp H_0$ dashed) for 1-mm-thick sample. Magnetic field, H_0 , is 15,000 oersteds. Parameters characterizing ferrite (TT2-111) are given in figure 1. (See fig. 9 for ϵ_2 .)

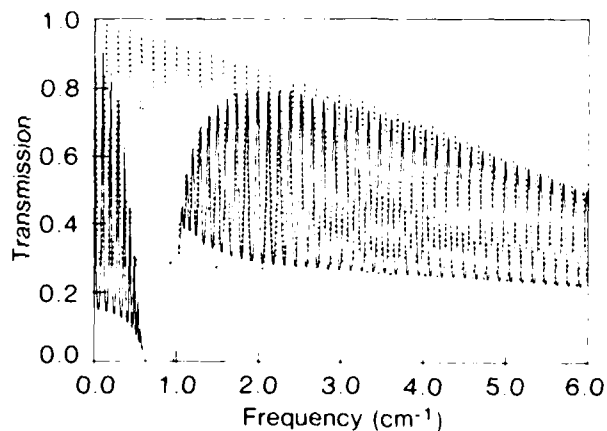


Figure 14. Power transmission coefficient ($E \parallel H_0$ solid, $E \perp H_0$ dashed) for 1-cm-thick sample. Magnetic field, H_0 , is 5000 oersteds. Parameters characterizing ferrite are given in figure 1. (See fig. 9 for ϵ_2 .)

3. DISCUSSION AND CONCLUSION

We have investigated in detail both the frequency region of ferromagnetic resonance and the region above resonance for a typical ferromagnetic material (TT2-111). In order to investigate the region near resonance with any precision experimentally, the spectrometer (or other frequency source--a stabilized source) must have very high resolution ($\Delta\nu < \gamma\Delta H$). The ferrite chosen for many of the calculations required a field of 50,000 oersteds for resonance at $\sim 5 \text{ cm}^{-1}$. This handicap can be overcome somewhat by using barium ferrite. For barium ferrite with $H_A \approx 18,000$ oersteds, the external magnetic field H_0 is $H_0 \approx 50,000 - H_A \approx 32,000$ oersteds (Van Aulock--p 464).⁴ Nevertheless, some barium ferrites have a smaller ΔH than the prototype chosen here.⁴ Thus, the direct measurement of the properties of these ferrites near magnetic resonance requires very high resolution ($\Delta\nu \leq \gamma\Delta H/5 \approx 25 \text{ MHz}$) by the spectrometer or, if the measurements are made at constant frequency, the source must have a corresponding stability.

The frequency region above resonance was examined for the possibility of meaningful measurements. The results presented here tend to indicate that the spectrometer requirements are much less stringent. Meaningful measurements can be made on ferrite material developed for the microwave region by somewhat conventional Fourier transform spectrometers.

⁴W. H. Von Aulock, ed., Handbook of Microwave Ferrite Materials, Academic Press, New York (1965), 464.

Finally, in developing and checking the computer programs to calculate the results presented here, we are in a position to determine the experimental variables (sample thickness, external magnetic field, etc) necessary to make measurements on a particular ferrite. All that is necessary is a reasonable approximation to the real and imaginary parts of the dielectric constant and the anisotropy field, if appropriate.

Acknowledgements

We wish to thank Richard P. Leavitt for the use of his computer program and his help in how to run it.

LITERATURE CITED

- (1) George J. Simonis, Joseph P. Sattler, Terrance L. Worchesky, and Richard P. Leavitt, Characterization of Near-Millimeter Wave Materials by Means of Non-Dispersive Fourier Transform Spectroscopy, *J. Infrared and Mill. Waves* 5 (1984); 57. (This reference reports the measured complex dielectric constant of TT2-111, the prototype ferrite used here.) See also George J. Simonis, Index to the Literature Dealing with the Near-Millimeter Wave Properties of Materials, *Int. J. Infrared and Mill. Waves*, 3 (1982), 439 (170 articles referenced).
- (2) Clyde A. Morrison, A. F. Hansen, and K. M. Sorenson, Theoretical Analysis of Nonreciprocal Electromagnetic Surface Wave Devices, Harry Diamond Laboratories, HDL-TR-2017 (September 1983).
- (3) T. A. Gilbert, Armour Research Foundation, Rept. No. 11 (25 January 1955).
- (4) W. H. Von Aulock, ed., Handbook of Microwave Ferrite Materials, Academic Press, New York (1965).
- (5) Joseph Nemarich, Measurement of Narrow Magnetic Resonance Linewidths, Harry Diamond Laboratories, HDL-TR-1246 (10 August 1964).
- (6) C. Kittel, Introduction to Solid State Physics, Wiley and Sons, New York (1976).
- (7) Donald E. Wortman, L. A. Ault, and Clyde A. Morrison, Ferromagnetic Resonance from 300 MC to 10 kMC in Oriented YIG Discs, Harry Diamond Laboratories, HDL-TR-992 (8 November 1961).

DISTRIBUTION

ADMINISTRATOR
DEFENSE TECHNICAL INFORMATION CENTER
ATTN DTIC-DDA (12 COPIES)
CAMERON STATION, BUILDING 5
ALEXANDRIA, VA 22314

DIRECTOR
DEFENSE ADVANCED RESEARCH PROJECTS
AGENCY

ARCHITECT BLDG
ATTN MATERIALS SCIENCES
ATTN ADVANCED CONCEPTS DIV
ATTN TARGET ACQUISITION
& ENGAGEMENT DIV
ATTN TTO, DR. J. TEGNELIA
ATTN STO, DR. S. ZAKANYCZ
1400 WILSON BLVD
ARLINGTON, VA 22209

INSTITUTE FOR DEFENSE ANALYSIS
ATTN DR. V. J. CORCORAN
1801 N. BEAUREGARD ST
ALEXANDRIA, VA 22311

DIRECTOR
DEFENSE COMMUNICATIONS AGENCY
ATTN TECHNICAL LIBRARY
ATTN COMMAND & CONTROL CENTER
WASHINGTON, DC 20305

DIRECTOR
DEFENSE COMMUNICATIONS ENGINEERING
CENTER
ATTN TECHNICAL LIBRARY
1860 WIEHLE AVENUE
RESTON, VA 22090

DIRECTOR
NATIONAL SECURITY AGENCY
ATTN TECHNICAL LIBRARY
FT MEADE, MD 20755

OUSDR&E
DIRECTOR ENERGY TECHNOLOGY OFFICE
THE PENTAGON
WASHINGTON, DC 20301

OUSDR&E
ASSISTANT FOR RESEARCH
THE PENTAGON
WASHINGTON, DC 20301

OFFICE OF THE DEPUTY CHIEF OF STAFF
FOR RESEARCH, DEVELOPMENT, &
ACQUISITION
ATTN DIR OF ARMY RES, DAMA-ARZ-A
DR. M. E. LASSER
ATTN DAMA-E, ADVANCED CONCEPTS TEAM
WASHINGTON, DC 20310

COMMANDER
US ARMY ARMAMENT MATERIEL
READINESS COMMAND
ATTN DRSAR-LEP-L, TECHNICAL LIBRARY
ATTN DRSAR-ASF, FUZE & MUNITIONS
SUPPORT DIV
ROCK ISLAND, IL 61299

COMMANDER
US ARMY ATMOSPHERIC SCIENCES LABORATORY
ATTN DRSEL-BL-AS-P, DR. K. WHITE
WHITE SANDS MISSILE RANGE, NM 88002

COMMANDER
BALLISTIC MISSILE DEFENSE AGENCY
ADVANCED TECHNOLOGY CENTER
ATTN BMD-ATC-D, C. JOHNSON
PO BOX 1500
HUNTSVILLE, AL 35807

DIRECTOR
US ARMY BALLISTIC RESEARCH LABORATORY
ATTN DRDAR-TSB-S (STINFO)
ATTN DRDAR-BLB, R. MCGEE
ATTN DRDAR-BL, H. REED
ABERDEEN PROVING GROUND, MD 21005

COMMANDER
US ARMY COMMUNICATIONS & ELECTRONICS
MATERIEL READINESS COMMAND
ATTN H. JACOBS
ATTN V. G. GELNOVATCH
ATTN R. STERN
FT MONMOUTH, NJ 07703

COMMANDER
EDGEWOOD ARSENAL
ABERDEEN PROVING GROUND, MD 21005

DIRECTOR
ELECTRONIC WARFARE LABORATORY
ATTN DELEW-SM, EW SYSTEMS MGT OFFICE
ATTN DELEW-C, COMM INTEL/CM DIV
ATTN DELEW-E, ELCT INTEL/CM DIV
FT MONMOUTH, NJ 07703

COMMANDER/DIRECTOR
COMBAT SURVEILLANCE & TARGET
ACQUISITION LABORATORY
ATTN DELET-DD
ATTN DELCS-DT, CHIEF TECHNICAL PLANS &
MGT OFFICE
ATTN DELCS-R, DIR RADAR DIV
FT MONMOUTH, NJ 07703

COMMANDER
US ARMY ELECTRONICS PROVING GROUND
FT HUACHUCA, AZ 85613

DISTRIBUTION (cont'd)

COMMANDER/DIRECTOR
ATMOSPHERIC SCIENCES LABORATORY
US ARMY LABCOM
ATTN DELAS-EO, ELECTRO-OPTICS DIVISION
WHITE SANDS MISSILE RANGE, NM 88002

COMMANDER
LABCOM TECHNICAL SUPPORT ACTIVITY
ATTN DELSD-L, TECH LIB DIR
FT MONMOUTH, NJ 07703

DIRECTOR
ELECTRONICS TECHNOLOGY &
DEVICES LABORATORY
ATTN DELET-DT, DIR TECHNICAL PLANS &
PROGRAMS OFFICE
ATTN DELET-E, DIR ELECTRONIC MATERIALS
RESEARCH DIV
ATTN DELET-I DIR MICROELECTRONICS DIV
ATTN DELET-M, MICROWAVE & SIGNAL
PROCESSING DEVICES DIV
FT MONMOUTH, NJ 07703

COMMANDER
US ARMY LABCOM
ATTN DRSEL-TL-IJ, DR. A. KERECMAN
ATTN DRSEL-CT-R, R. PEARCE
ATTN DRSEL-CT-L, DR. ROHDE
FT MONMOUTH, NJ 07703

US ARMY FOREIGN SCIENCE & TECHNOLOGY
CENTER
ATTN DRXST-SD, DR. O. R. HARRIS
220 SEVENTH STREET, NE
CHARLOTTESVILLE, VA 22901

COMMANDER
US ARMY MATERIEL RESEARCH &
DEVELOPMENT COMMAND
DOVER, NJ 07801

COMMANDER
US ARMY INTELLIGENCE & SEC COMMAND
ATTN TECH LIBRARY
ARLINGTON HALL STATION
4000 ARLINGTON BLVD
ARLINGTON, VA 22212

COMMANDER
US ARMY MATERIEL COMMAND
ATTN DRCBSI, DR. P. DICKINSON
ATTN DRCPA, DIR FOR PLANS &
ANALYSIS
ATTN DRCDE, DIR FOR DEVELOPMENT & ENG
5001 EISENHOWER AVE
ALEXANDRIA, VA 22333-0001

COMMANDER
US ARMY MATERIALS & MECHANICS
RESEARCH CENTER
ATTN DRXMR-PL, TECHNICAL LIBRARY
WATERTOWN, MA 02172

DIRECTOR
US ARMY MATERIEL SYSTEMS ANALYSIS
ACTIVITY
ATTN DRXSY-MP
ABERDEEN PROVING GROUND, MD 21005

COMMANDER
US ARMY MIRADCOM
ATTN DRDMI-TRO, DR. W. L. GAMBLE
ATTN DRDMI-TRO, DR. B. D. GUENTHER
ATTN DRSMI-REO, DR. G. EMMONS
REDSTONE ARSENAL, AL 35809

COMMANDER
US ARMY MISSILE COMMAND
ATTN DRSMI-RLA, K. LETSON
ATTN DRSMI-RLA, D. HARTMAN
REDSTONE ARSENAL, AL 35898

COMMANDER
US ARMY MISSILE & MUNITIONS
CENTER & SCHOOL
ATTN ATSK-CTD-F
REDSTONE ARSENAL, AL 35809

COMMANDER
US ARMY NATICK RES & DEV COMMAND
NATICK DEVELOPMENT CENTER
ATTN DRDNA-T, TECHNICAL LIBRARY
NATICK, MA 01760

DIRECTOR
NIGHT VISION & ELECTRO-OPTICS
LABORATORY
ATTN DELNV-IRT, INFRARED TECHNOLOGY DIV
ATTN DELNV-L, LASER DIVISION
ATTN DELNV-L, DR. R. G. BUSER
ATTN DELNV-R, ELECTRO-OPTICS RES
ATTN DELNV-R, ELECTRONICS MATERIALS RES
ATTN DELNV-SI, OPTICS
ATTN DELNV-SI, ELECTRONICS
ATTN DRSEL-NV-VI, J. R. MOULTON
ATTN DRSEL-NV-VI, DR. R. SHURTZ
FT BELVOIR, VA 22060

COMMANDER
US ARMY NUCLEAR & CHEMICAL AGENCY
ATTN ATCN-W, WEAPONS EFFECTS DIV
7500 BACKLICK ROAD
BUILDING 2073
SPRINGFIELD, VA 22150

DISTRIBUTION (cont'd)

COMMANDER/DIRECTOR
CHEMICAL SYSTEMS LABORATORY
ARRADCOM
ATTN DRDAR-CLJ-L, TECHNICAL LIBRARY BRANCH
ABERDEEN PROVING GROUND, MD 21010

DIRECTOR
US ARMY RESEARCH & TECHNOLOGY
LABORATORIES
AMES RESEARCH CENTER
MOFFETT FIELD, CA 94035

US CHIEF ARMY RESEARCH OFFICE (DURHAM)
PO BOX 12211
ATTN DRXRO-EL, DIR ELECTRONICS DIV
ATTN DRXRO-PH, DIR PHYSICS DIV
ATTN DRXRO-MS, METALLURGY-MATERIALS
DIV
RESEARCH TRIANGLE PARK, NC 27709

DIRECTOR
PROPULSION LABORATORY
RESEARCH & TECHNOLOGY LABORATORIES
AVRADCOM
LEWIS RESEARCH CENTER, MS. 106-2
21000 BROOKPARK ROAD
CLEVELAND, OH 44135

DIRECTOR
APPLIED TECHNOLOGY LABORATORY
AVRADCOM
ATTN DAVDL-ATL-TSD, TECH LIBRARY
FT EUSTIS, VA 23604

ASSISTANT SECRETARY OF THE NAVY
RESEARCH, ENGINEERING, & SYSTEMS
DEPT OF THE NAVY
WASHINGTON, DC 20350

CHIEF OF NAVAL RESEARCH
DEPT OF THE NAVY
ATTN ONR-400, ASST CH FOR RES
ATTN ONR-420, PHYSICAL SCI DIV
ARLINGTON, VA 22217

COMMANDER
NAVAL RESEARCH LAB
ATTN B. YAPLEE, CODE 7110
ATTN DR. J. P. HOLLINGER, CODE 7111
ATTN DR. K. SHIVANANDAN, CODE 7122.1
WASHINGTON, DC 20375

SUPERINTENDENT
NAVAL POSTGRADUATE SCHOOL
ATTN LIBRARY, CODE 2124
MONTEREY, CA 93940

DIRECTOR
NAVAL RESEARCH LABORATORY
ATTN 2600, TECHNICAL INFO DIV
ATTN 2750, OPTICAL SCIENCES DIV
ATTN 5500, OPTICAL SCI DIV
ATTN 6000, MATL & RADIATION
SCI & TE
WASHINGTON, DC 20375

COMMANDER
NAVAL SURFACE WEAPONS CENTER
ATTN DX-21, LIBRARY DIV
DAHLGREN, VA 22448

COMMANDING OFFICER
NAVAL TRAINING EQUIPMENT CENTER
ATTN TECHNICAL LIBRARY
ORLANDO, FL 32813

COMMANDER
NAVAL WEAPONS CENTER
ATTN 38, RESEARCH DEPT
ATTN 381, PHYSICS DIV
CHINA LAKE, CA 93555

HQ, USAF/SAMI
WASHINGTON, DC 20330

DEPUTY CHIEF OF STAFF
RESEARCH & DEVELOPMENT
HEADQUARTERS, US AIR FORCE
ATTN AFRDQSM
WASHINGTON, DC 20330

SUPERINTENDENT
HQ US AIR FORCE ACADEMY
ATTN TECH LIB
USAF ACADEMY, CO 80840

COMMANDER
AIR FORCE AVIONICS LABORATORY
ATTN KJA (TEO), ELECTRO-OPTICS
TECHNOLOGY BR
WRIGHT-PATTERSON AFB, OH 45433

HQ AF DATA AUTOMATION AGENCY
ATTN DATA SYS EVAL OFFICE
GUNTER AFS, AL 36114

COMMANDER
HQ ROME AIR DEVELOPMENT CENTER (AFSC)
ATTN LE, DEPUTY FOR ELECTRONIC TECH
ATTN LMT, TELECOMMUNICATIONS BR
GRIFFISS AFB, NY 13441

COMMANDER
US AIR FORCE GEOPHYSICAL LAB
L. G. HANSCOMB FIELD
ATTN DR. S. A. CLOUGH
BEDFORD, MA 01731

DISTRIBUTION (cont'd)

DIRECTOR
AF OFFICE OF SCIENTIFIC RESEARCH
BOLLING AFB
ATTN NE, DIR OF ELECTRONIC &
SOLID STATE SCI
WASHINGTON, DC 20332

COMMANDER
US AIR FORCE ROME AIR DEVELOPMENT
CENTER
ATTN RADC/ETEN, DR. E. ALTSHULER
L. G. HANSCOM FIELD
BEDFORD, MA 01730

COMMANDER
HQ AIR FORCE SYSTEMS COMMAND
ANDREWS AFB
ATTN TECHNICAL LIBRARY
WASHINGTON, DC 20334

AF WEAPONS LABORATORY, AFSC
ATTN EL, ELECTRONICS DIV
ATTN LR, LASER DEV DIV
KIRTLAND AFB, NM 87117

AMES RESEARCH CENTER
NASA
ATTN TECHNICAL INFO DIV
MOFFETT FIELD, CA 94035

DIRECTOR
NASA
GODDARD SPACE FLIGHT CENTER
ATTN 250, TECH INFO DIV
GREENBELT, MD 20771

DIRECTOR
NASA
ATTN TECHNICAL LIBRARY
JOHN F. KENNEDY SPACE
CENTER, FL 32899

DIRECTOR
NASA
LANGLEY RESEARCH CENTER
ATTN TECHNICAL LIBRARY
HAMPTON, VA 23665

DIRECTOR
NASA
LEWIS RESEARCH CENTER
ATTN TECHNICAL LIBRARY
CLEVELAND, OH 44135

DEPARTMENT OF COMMERCE
NATIONAL BUREAU OF STANDARDS
ATTN LIBRARY
WASHINGTON, DC 20230

NATIONAL OCEANIC & ATMOSPHERIC ADM
ENVIRONMENTAL RESEARCH LABORATORIES
ATTN LIBRARY, R-51, TECH REPORTS
BOULDER, CO 80302

INSTITUTE FOR TELECOMMUNICATIONS
SCIENCES
NATIONAL TELECOMMUNICATIONS &
INFO ADMIN
ATTN LIBRARY
BOULDER, CO 80303

THE AEROSPACE CORPORATION
THE IVAN A. GETTING LAB
ATTN DR. T. S. HARTWICK
ATTN DR. D. T. HODGES
PO BOX 92957
LOS ANGELES, CA 90009

ENGINEERING SOCIETIES LIBRARY
ATTN ACQUISITIONS DEPARTMENT
345 EAST 47TH STREET
NEW YORK, NY 10017

ENVIRONMENTAL RESEARCH INSTITUTE OF
MICHIGAN
ATTN DR. GWYNN H. SUITS
PO BOX 618
ANN ARBOR, MI 48107

FORD-AERONUTRONIC
ATTN DR. D. E. BURCH
FORD ROAD
NEWPORT BEACH, CA 92663

HONEYWELL CORPORATE RESEARCH CENTER
ATTN DR. P. W. KRUSE
10701 LYNDAL AVE S
BLOOMINGTON, MN 55420

LAWRENCE LIVERMORE NATIONAL LABORATORY
PO BOX 808
LIVERMORE, CA 94550

MARTIN MARIETTA
ATTN R. P. LEAVITT, 13200
1450 SOUTH ROLLING RD
BALTIMORE, MD 21227

NATIONAL OCEANOGRAPHIC & ATMOSPHERIC
ADMINISTRATION
ATTN DR. V. E. DERR
BOULDER, CO 80303

R&D ASSOCIATES
ATTN R. G. GORDON
PO BOX 9695
MARIETTA DEL REY, CA 90291

DISTRIBUTION (cont'd)

SANDIA LABORATORIES
LIVERMORE LABORATORY
PO BOX 969
LIVERMORE, CA 94550

SANDIA NATIONAL LABORATORIES
PO BOX 5800
ALBUQUERQUE, NM 87185

JET PROPULSION LABORATORY
CALIFORNIA INSTITUTE OF TECHNOLOGY
4800 OAK GROVE DRIVE
ATTN TECHNICAL LIBRARY
PASADENA, CA 91103

GEORGIA INSTITUTE OF TECHNOLOGY
ENGINEERING EXPERIMENT STATION
ATTN J. J. GALLAGHER
ATLANTA, GA 30332

UNIVERSITY OF CALIFORNIA
SCHOOL OF ENGINEERING
LOS ANGELES, CA 90024

UNIVERSITY OF ILLINOIS
DEPT OF ELECTRICAL ENGINEERING, 200 EERL
ATTN DR. P. D. COLEMAN
ATTN DR. T. A. DETEMPLE
URBANA, IL 61801

MIT
FRANCIS BITTER NATIONAL MAGNET LAB
ATTN K. J. BUTTON
170 ALBANY STREET
CAMBRIDGE, MA 02139

MIT
LINCOLN LAB
ATTN C. BLAKE
PO BOX 73
LEXINGTON, MA 02173

CIVIL ENGINEERING RESEARCH FACILITY
UNIVERSITY OF NEW MEXICO
PO BOX 188
ALBUQUERQUE, NM 87131

RUTGERS UNIVERSITY
COLLEGE OF ENGINEERING
DEPARTMENT OF CERAMICS
NEW BRUNSWICK, NJ 08903

US ARMY LABORATORY COMMAND
ATTN COMMANDER, AMSLC-CG
ATTN TECHNICAL DIRECTOR, AMSLC-TD

INSTALLATION SUPPORT ACTIVITY
ATTN DIVISION DIRECTOR, SLCIS-D
ATTN RECORD COPY, SLCIS-IM-TS
ATTN LIBRARY, SLCIS-IM-TL (3 COPIES)
ATTN LIBRARY, SLCIS-IM-TL (WOODBIDGE)
ATTN TECHNICAL REPORTS BRANCH, SLCIS-IM-TR
ATTN LEGAL OFFICE, SLCIS-CC
ATTN S. ELBAUM, SLCIS-CC-IP

HARRY DIAMOND LABORATORIES
ATTN D/DIVISION DIRECTORS
ATTN DIVISION DIRECTOR, SLCHD-RT
ATTN J. P. SATTLE, SLCHD-PO-P
ATTN CHIEF, SLCHD-NW-P
ATTN H. E. BRANDT, SLCHD-NW-RI
ATTN B. ZABLUDOWSKI, SLCHD-IT-EB
ATTN C. LANHAM, SLCHD-TT
ATTN W. TRUEHART, SLCHD-RT-AA
ATTN F. G. FARRAR, SLCHD-RT-AB
ATTN W. G. WIEBACH, SLCHD-RT-AB
ATTN S. M. KULPA, SLCHD-RT-AC
ATTN J. NEMARICH, SLCHD-RT-AC
ATTN B. A. WEBER, SLCHD-RT-AC
ATTN Z. G. SZTANKAY, SLCHD-RT-AC
ATTN B. J. BENCIVENGA, SLCHD-RT-AD
(10 COPIES)

ATTN J. F. DAMMANN, SLCHD-RT-AD
ATTN J. SELTZER, SLCHD-RT-AD
ATTN P. S. BRODY, SLCHD-RT-RA
ATTN H. DROPKIN, SLCHD-RT-RA
ATTN G. T. SIMONIS, SLCHD-RT-RA
(30 COPIES)

ATTN M. S. TOBIN, SLCHD-RT-RA
ATTN D. E. WORTMAN, SLCHD-RT-RA
ATTN D. GIGLIO, SLCHD-RT-RC
ATTN C. A. MORRISON, SLCHD-RT-RA
(10 COPIES)